

Spin-filtering effect in the transport through a single-molecule magnet Mn_{12} bridged between metallic electrodes

Salvador Barraza-Lopez^{1*}, Kyungwha Park¹, Víctor García-Suárez², and Jaime Ferrer³

¹*Department of Physics, Virginia Polytechnic Institute and State University. Blacksburg VA, 24061*

²*Department of Physics, Lancaster University, Lancaster, LA1 4YB, United Kingdom*

³*Departamento de Física, Universidad de Oviedo, 33007 Oviedo, Spain*

(Dated: October 19, 2018)

Abstract

Electronic transport through a single-molecule magnet Mn_{12} in a two-terminal set up is calculated using the non-equilibrium Green's function method in conjunction with density-functional theory. A single-molecule magnet Mn_{12} is bridged between Au(111) electrodes via thiol group and alkane chains such that its magnetic easy axis is normal to the transport direction. A computed spin-polarized transmission coefficient in zero-bias reveals that resonant tunneling near the Fermi level occurs through some molecular orbitals of majority spin only. Thus, for low bias voltages, a spin-filtering effect such as only one spin component contributing to the conductance, is expected. This effect would persist even with inclusion of additional electron correlations.

PACS numbers: 72.25.-b, 73.63.-b, 75.50Xx, 71.15Mb

* Present address: School of Physics, Georgia Institute of Technology, Atlanta, GA 30332

Electronic transport through single-molecule magnets (SMMs) has recently been measured in three-terminal setups or using scanning tunneling microscope (STM).^{1,2,3,4} Both of the experimental techniques face their own challenges in transport measurements, so do theoretical and computational studies of the systems. So far, there were no experimental or theoretical inputs on the interfaces between SMMs and electrodes. It is also extremely difficult to control these interfaces. SMMs can be differentiated from organic molecules in the sense that they have large magnetic moments and large magnetic anisotropy barriers caused by spin-orbit coupling. In addition, SMMs differ from magnetic clusters comprising magnetic elements only because the magnetic ions in SMMs are interacting with each other via organic/inorganic ligands. It was shown that the magnetic properties of SMMs change significantly with the number of extra electrons added to the molecules,^{5,6} which may greatly impact their transport properties. Several theoretical studies^{7,8,9} on the transport through SMMs, have been, so far, based on many-body model Hamiltonians considering an important role of strong correlations in SMMs. However, in these model Hamiltonian studies, effects of interfaces and molecular geometries that also play a crucial role in transport were not properly included. In this sense, first-principles calculations could complement the existing many-body Hamiltonian studies.

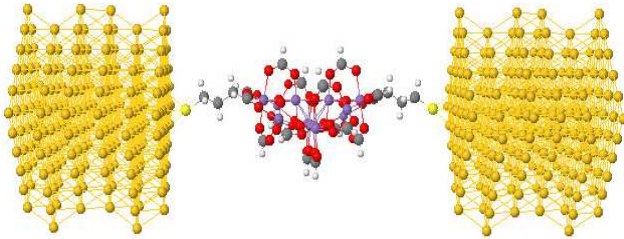


FIG. 1: (Color online). Extended molecule or scattering region consisting of SMM Mn_{12} (center) attached to Au layers via S atoms and alkane chains. Semi-infinite Au electrodes are considered in the calculations (not shown).

In this work, we present first-principles calculations of transport properties through a SMM Mn_{12} when the molecule is bridged between Au(111) electrodes. We identify plausible pathways of the transport within the molecule and find a spin-filtering effect in the transport caused by the nature of Mn_{12} molecular orbitals responsible for resonant tunneling. For this study, we use the non-equilibrium Green's function method and the density-functional

theory (DFT), with the SIESTA-based¹⁰ quantum transport code, SMEAGOL.^{11,12} To include additional electron correlations, we also add a Hubbard-like U term to our DFT calculations using VASP¹³. Our main results reported in this work do not change with the addition of U term except for an increased HOMO-LUMO gap comparable to the experimental value.⁴ In our study the following assumptions are made: (1) Despite intermediate transient states, the system eventually reaches the stable state. (2) Currents can be obtained from the methodology based on the ground-state DFT even when a bias voltage is applied. (3) Interactions of molecules with heat baths are not included. As discussed in Ref.11, we divide the whole system into two parts: (i) bulk left and right Au electrodes, and (ii) a scattering region consisting of several Au layers, a SMM Mn₁₂, and two linker molecules (S atoms and alkane chains). The scattering region [also called extended molecule (EM)] is shown in Fig.1. The bulk electrodes are treated semi-infinite and their electronic structures are computed using SIESTA. A current is expressed as¹⁴ $I = (e/h) \int dE T(E, V)(f(E - \mu_L) - f(E - \mu_R))$, where $T(E, V)$ is a transmission coefficient, V is a bias voltage, and $f(E - \mu_L)$ and $f(E - \mu_R)$ are the Fermi functions for the left and right electrodes with chemical potentials μ_L and μ_R , respectively. $T(E, V)$ can be cast as

$$T(E, V) = \Gamma_L(E, V)G_M^\dagger(E, V)\Gamma_R(E, V)G_M(E, V) \quad (1)$$

where $\Gamma_{L,R}$ is the density of states of the left or right electrode and G_M is the Green's function of the EM. Within the non-equilibrium Green's function method, G_M is solved self-consistently in the context of the DFT.

For spin-polarized DFT calculations with SIESTA we use Perdew-Burke-Ernzerhof (PBE) generalized-gradient approximation (GGA)¹⁵ for exchange-correlation potential. We generate Troullier-Martins pseudopotentials¹⁶ for Au, Mn, S, O, C, and H with scalar relativistic terms and core corrections except for H, as well as basis sets for each element. For Mn atoms 3p orbitals are included in the valence states. For an isolated Mn₁₂ the molecular orbitals near the Fermi level obtained using the generated basis sets and pseudopotentials agree well within 0.1 eV with those using other DFT codes such as NRLMOL¹⁷ and VASP. We also compute the magnetic anisotropy barrier for Mn₁₂ by including the spin-orbit interaction self-consistently in DFT calculations with a version of SIESTA that includes spin-orbit coupling¹². The barrier we obtain agrees with the experimental value¹⁸. All of these tests reveal that our generated pseudopotentials and basis sets are good enough to study the

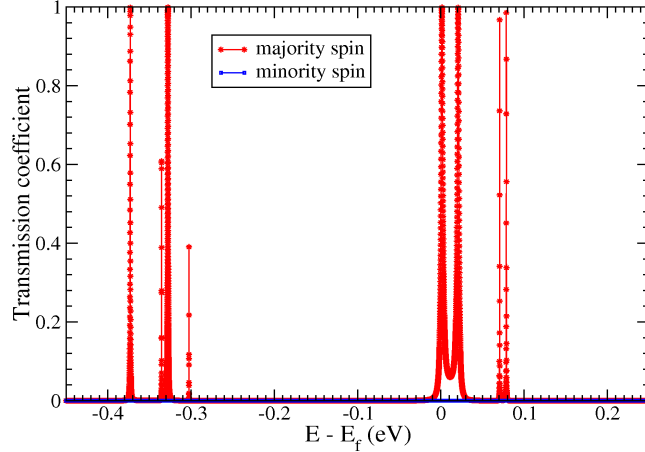


FIG. 2: (Color online). Spin-polarized transmission coefficient in zero bias.

system of interest.

To construct the bulk leads, we use an optimum bulk lattice constant of 4.166 Å, resulting in a vertical distance between adjacent layers of 2.405 Å. The electronic structure and self-energies of Au(111) electrodes are computed using SIESTA. For the EM we consider a geometry in which a Mn₁₂ molecule is oriented such that its magnetic easy axis is normal to the transport direction (z axis) and in which six Au layers are included on each side of the Mn₁₂ molecule (Fig. 1). This geometry completely covers a Mn₁₂ molecule and prevents different Mn₁₂ molecules from interacting with each other. Mn₁₂ molecules are not directly chemically bonded to Au, and so thiol groups and alkane chains are used to attach Mn₁₂ to Au (Fig. 1). In the EM, $3 \times 3 \times 1$ k points are sampled. The periodic boundary conditions are imposed on the EM along all directions to self-consistently solve for the Green's function of the EM.

The computed spin-polarized transmission coefficient in zero bias is shown as a function of energy relative to the Fermi level E_f in Fig. 2. The peaks in the transmission coefficient are very narrow due to weak coupling between the electrodes and Mn₁₂, as discussed in our previous DFT calculation.¹⁹ Thus, one can identify a one-to-one mapping between individual transmission peaks and molecular orbitals. The transmission coefficient from minority-spin electrons is zero in the energy region shown in Fig. 2. The first minority-spin transmission peak appears at 0.71 eV above E_f . So contributions to the transmission near E_f are from majority-spin electrons only. This is because only majority-spin molecular orbitals are near

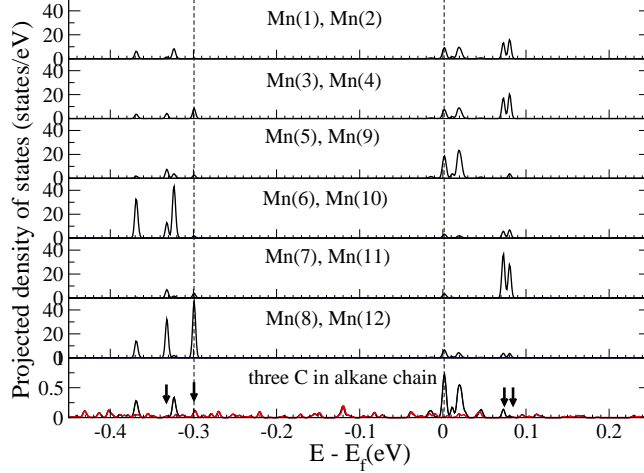


FIG. 3: (Color online). Spin-polarized density of states of the EM projected onto Mn d and C p orbitals (majority spin: black, minority spin: red). Minority-spin densities for Mn are zero in the energy range shown. The Mn ions are labeled in Fig. 4. The dashed lines (arrows) are for the HOMO and LUMO (HOMO-2, HOMO, LUMO+2, LUMO+3) of Mn_{12} from the left. The LUMO is slightly above the Fermi level.

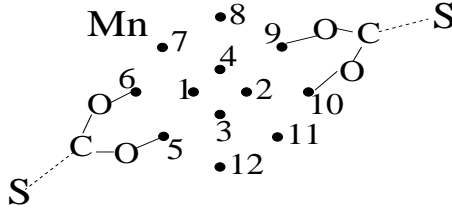


FIG. 4: Positions of Mn ions (filled circles), few O, C, and S atoms. The dashed lines represent the alkane chains. The S atoms are directly bonded to the Au leads.

E_f and they are well separated from minority-spin molecular orbitals. This feature may be seen in the spin-polarized projected density of states onto Mn d and C p orbitals (Figs. 3 and 4). The minority-spin densities of Mn d orbitals are zero in the energy range shown in Fig. 3. Compared to fourfold symmetric Mn d orbitals in an isolated Mn_{12} , the Mn d orbitals in the EM reveal twofold symmetry because of broken symmetry caused by the leads (Fig. 3). By comparing Fig. 3 to Fig. 2, we find that the four transmission peaks between $E=0$ and 0.1 eV are from the majority-spin lowest-unoccupied-molecular-orbital (LUMO) and the three levels right above the LUMO (LUMO+n, $n=1,2,3$), while the four peaks between $E=-0.4$ and -0.3 eV are from the majority-spin highest-occupied-molecular-

orbital (HOMO) and the three levels right below the HOMO (HOMO- n , $n=1,2,3$). The HOMO is mainly from Mn(8) and Mn(12) and the HOMO-1 and HOMO-3 are from Mn(6) and Mn(10). The LUMO and LUMO+1 are from Mn(5) and Mn(9) and the LUMO+2 and LUMO+3 are from Mn(7) and Mn(11). Although a corresponding transmission peak appears at the energy level of each molecular orbital in the range, not all of the orbitals would significantly contribute to the current because of the extremely narrow widths of peaks. The peaks at $E=-0.335$, -0.35 , 0.07 , and 0.08 eV, have widths of less than 10^{-5} eV, and so they would not contribute much to the current. The widths of transmission peaks depend on the extent of the electron density overlap or level broadening along the transport pathways. For example, for electrons to be transmitted through Mn₁₂, they must tunnel through the alkane chains. The spin-polarized density of states projected onto the three C atoms in each alkane chain shows small peaks at the energies of the HOMO-2, HOMO, LUMO+2, LUMO+3 as indicated by the arrows in the bottom panel of Fig. 3, resulting in extremely narrow transmission peaks. Thus, more electrons would tunnel through the LUMO, LUMO+1, HOMO-1, and HOMO-3.

For comparison with experimental data, strong correlation effects which are lacking in GGA, should be included. Insight on these effects on transport is provided from GGA+U studies on an isolated Mn₁₂. Our previous GGA+U study on a neutral Mn₁₂²⁰ suggests that the HOMO-LUMO gap shown in Figs. 2 and 3 would increase so that a higher bias voltage would be needed to charge the Mn₁₂ molecule than appeared in Fig. 2. However, with a downward shift of occupied levels and upward shift of unoccupied levels, the main features including spin filtering would persist. When the Mn₁₂ molecule is singly charged with inclusion of U , we find that the level corresponding to the LUMO of the neutral Mn₁₂ is now filled so that the energy gap for the charged Mn₁₂ becomes very small. Thus, what we learned from the zero-bias case would be still relevant for non-zero bias cases to large extent. Further studies on the charged Mn₁₂ molecule in transport are in progress.

In summary, we have investigated transport properties through a Mn₁₂ molecule bridged between Au(111) electrodes using the non-equilibrium Green's function method and spin-polarized DFT. We found that a spin-filtering effect occurs in the transmission for non-ferromagnetic electrodes. In addition, not all of the molecular orbitals near E_f involved with the resonant tunneling, equally contribute to the current.

K.P. was supported by the Jeffress Memorial Trust Funds and NSF DMR-0804665. J.F.

was supported by MEC FIS2006-12117. Computational support was provided by the SGI Altix Linux Supercluster at the National Center for Supercomputing Applications under DMR060009N and by Virginia Tech Linux clusters and Advanced Research Computing.

- ¹ H. B. Heersche, Z. de Groot, J. A. Folk, H. S. van der Zant, C. Romeike, M. R. Wegewijs, L. Zobbi, D. Barreca, E. Tondello, and A. Cornia, *Phys. Rev. Lett.* **96**, 206801 (2006)
- ² M.-H. Jo, J. E. Grose, K. Baheti, M. M. Deshmukh, J. J. Sokol, E. M. Rumberger, D. N. Hendrickson, J. R. Long, H. Park, and D. C. Ralph, *Nano Lett.* **6**, 2014 (2006).
- ³ J.J. Henderson, C.M. Ramsey, E. del Barco, A. Mishra, and G. Christou, *J. Appl. Phys.* **101**, 09E102 (2007).
- ⁴ S. Voss, M. Fonin, U. Rudiger, M. Burgert, and U. Groth, *Appl. Phys. Lett.* **90**, 133104 (2007).
- ⁵ K. Park and M. R. Pederson, *Phys. Rev. B* **70**, 054414 (2004).
- ⁶ H. J. Eppley *et al.*, *J. Am. Chem. Soc.* **117**, 301 (1995); S.M.J. Aubin *et al.*, *Inorg. Chem.* **38**, 5329 (1999).
- ⁷ G.-H. Kim and T.-S. Kim, *Phys. Rev. Lett.* **92**, 137203 (2004).
- ⁸ C. Romeike, M. R. Wegewijs, and H. Schoeller, *Phys. Rev. Lett.* **96**, 196805 (2006).
- ⁹ F. Elste and C. Timm, *Phys. Rev. B* **73**, 235305 (2006).
- ¹⁰ J. M. Soler *et al.*, *J. Phys.: Condens. Matter* **14**, 2745 (2002); J. Junquera *et al.*, *Phys. Rev. B* **64**, 235111 (2001); P. Ordejón *et al.*, *Phys. Rev. B* **51**, 1456 (1995).
- ¹¹ A.R. Rocha, V.M. García-Suárez, S. Bailey, C. Lambert, J. Ferrer, and S. Sanvito, *Phys. Rev. B* **73**, 085414 (2006).
- ¹² L. Fernández-Seivane, M. A. Oliveira, S. Sanvito, and J. Ferrer, *J. Phys.: Condens. Matter* **18**, 7999 (2006).
- ¹³ G. Kresse and J. Furthmüller, *Phys. Rev. B* **54**, 11169 (1996); G. Kresse and J. Furthmüller, *Comp. Mat. Sci.* **6**, 15 (1996).
- ¹⁴ Y. Meir and N. S. Wingreen, *Phys. Rev. Lett.* **68**, 2512 (1992).
- ¹⁵ J. P. Perdew, K. Burke, and M. Ernzerhof, *Phys. Rev. Lett.* **77**, 3865 (1996).
- ¹⁶ N. Troullier and J. L. Martins, *Phys. Rev. B* **43**, 1993 (1991).
- ¹⁷ M. R. Pederson and K. A. Jackson, *Phys. Rev. B* **41**, 7453 (1990); K. A. Jackson and M. R. Pederson, *ibid.* **42**, 3276 (1990); D. V. Porezag, Ph.D. thesis, Chemnitz Technical Institute,

1997.

¹⁸ A. L. Barra, D. Gatteschi, and R. Sessoli, *Phys. Rev. B* **56**, 8192 (1997).

¹⁹ S. Barraza-Lopez, M. C. Avery, and K. Park, *Phys. Rev. B* **76**, 224413 (2007).

²⁰ S. Barraza-Lopez, M. C. Avery, and K. Park, *J. Appl. Phys.* **103**, 07B907 (2008).